

Seismic Imaging of Synthetic Data from a Physical Modelling Facility Channel Model

Xiaohui Cai¹, Kristopher Innanen¹, Daniel Trad¹, Joe Wong¹

¹ Department of Earth, Energy, and Environment, CREWES Project, University of Calgary

Summary

Full-Waveform Inversion (FWI) is a powerful seismic imaging technique capable of delivering high-resolution subsurface characterizations (Lailly and Bednar, 1983; Tarantola, 1984; Pratt, 1990; Virieux and Operto, 2009; Pan et al., 2020; Huang et al., 2021; Vigh et al., 2023). While its potential in complex geological scenarios is well-established, challenges remain in its application to simpler models, due to issues like dependence on low-frequency data and vulnerability to local minima. This study aims to develop an efficient and accurate FWI workflow adaptable to a variety of models. A frequency-domain multiscale FWI approach was employed to evaluate its ability to recover channel geometry, interface features, and internal velocity distributions. Results demonstrate that integrating low-frequency information and adopting a progressive frequency strategy are critical for enhancing inversion stability and accuracy. This work provides a foundation for robust FWI methodologies applicable to both physical modeling data and real-world seismic datasets.

Physical modeling data

CREWES conducted a 2D marine seismic survey at its seismic physical modeling laboratory (Figure 1). Data acquisition is managed by a two-dimensional gantry system, which is equipped with two eight-axis linear motors. This system is controlled by a motor drive controller identified as ACR-9600 and powered by a 24 V DC supply (Figure 1A). This setup ensures precise positioning and high-resolution data collection. The facility also includes arrays of small ultrasonic source and detector transducers (shown in Figure 1B), along with enhanced circuits for driving the source transducers, amplifying detected signals, and digitizing these signals. The physical model used in this study consists of three layers: a water layer, a PVC layer (illustrated in Figure 1C), and an acrylic Plexiglas (PLX) layer that contains an embedded channel structure (depicted in Figure 1D and E). The overall dimensions of the model are 2500 m horizontally and 1600 m vertically (Figure 2). The P-wave velocities for the layers are as follows: 1450 m/s in the water layer, 2350 m/s in the PVC layer, and 2750 m/s in the PLX layer. The embedded channel structure is completely housed within the PLX layer.

To simulate real-world seismic conditions, the physical modeling setup is scaled to a 1:10,000 ratio, with geological and acquisition parameters adjusted accordingly. After scaling, the acquisition geometry (see Figure 2) includes a source spacing of 50 meters and a receiver spacing of 10 meters, replicating a realistic seismic survey layout. Figure 3 presents the seismic shot obtained from the physical modeling experiment. The data exhibit a dominant frequency of 500 kHz, which is scaled down to 50 Hz during the scaling process, matching the typical frequency range observed in field seismic surveys.

The frequency requirements for accurately reconstructing the true model are derived based on the model's geological characteristics. With a minimum velocity of about 1500 m/s in the water layer, the relevant wavelengths needed to resolve critical features exceed 300 meters. The

dominant frequency required for long-wavelength information is calculated as 5 Hz. This highlights the importance of low-frequency content in providing long-wavelength updates critical for FWI. This study employs synthetic data generated under these controlled laboratory conditions to systematically evaluate the effectiveness of FWI in recovering channel geometries, interface features, and velocity distributions. By closely replicating both the acquisition geometry and the physical properties of the laboratory model, the synthetic data bridge the gap between theoretical studies and practical applications, offering valuable insights into the robustness and accuracy of FWI methods.

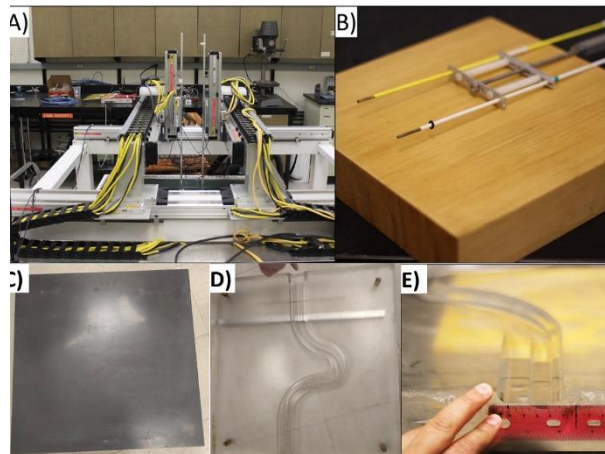


Figure 1. A) CREWES physical modelling laboratory facility. B) Source and receiver transducer. C) PVC Layer. D) PLX layer. E) Acrylic slab with a cut channel. Photographs courtesy of Joe Wong and Kevin Bertram.

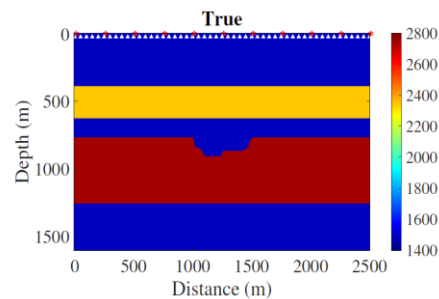


Figure 2. True velocity model and geometry, the red stars are the shots and white triangles are the receivers.

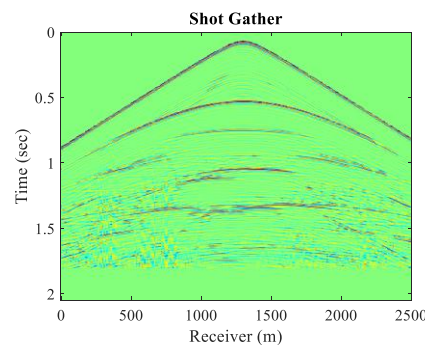


Figure 3. Seismic shot from physical modeling.

FREQUENCY-DOMAIN FWI

This synthetic study evaluates the effectiveness of FWI in recovering subsurface structures using two grid resolutions. A coarse grid ($dx = dz = 40m$) was used for initial testing and analysis, while a finer grid ($dx = dz = 10m$) was employed for high-resolution inversion. The inversion used a source wavelet with a dominant frequency of 50 Hz, consistent with the physical modelling experiment.

Two inversion strategies were tested: single-scale (Figure 4) and multiscale (Figure 5). The single-scale inversion used the full frequency range (1- 25 Hz) in a single step, while the multiscale approach incorporated each frequency band sequentially to progressively enhance resolution and convergence. Initial coarse-grid analysis revealed that frequencies below 9 Hz were effective in resolving large-scale structures, while frequencies above 9 Hz enhanced the recovery of fine-scale details, such as channel boundaries. The single-scale FWI results (Figure 4) failed to update the velocity structures, which illustrates that the reason conventional FWI fails to produce reasonable results for the channel model is the necessity of introducing low-frequency information first. In contrast, the multiscale inversion (Figure 5) demonstrated significant improvements, effectively capturing both large-scale structures and finer details. Gradual frequency incorporation allowed for better resolution of channel boundaries and velocity variations within the PLX layer. Based on these findings, a stepwise multiscale strategy was designed for the fine-grid model with five progressively expanding frequency bands: 1-6 Hz, 1-11 Hz, 1-15 Hz, 1-17 Hz, and 1-25 Hz. Each band involved 15 iterations, with the results from one band serving as the starting model for the next. Figure 6 shows the final inversion velocity. Velocity profiles extracted along two traces ($x = 620m$ and $x = 1240m$) provide a quantitative comparison between the true, initial, and inverted models (Figure 6). These profiles demonstrate that the fine-grid inversion closely matches the true model, particularly in the channel regions and at layer interfaces, with sharper transitions and improved detail compared to the coarse-grid results. These results validate the robustness of the multiscale FWI strategy in achieving both stability and resolution.

To validate the accuracy of the inverted velocity model, RTM was applied to both the initial and final inverted models, as shown in Figure 7. The RTM image derived from the initial model shows significant artifacts, particularly around the concave channel structure, where the reflectors are poorly imaged. In contrast, the RTM image based on the inverted model demonstrates clear improvements, with well-defined channel features and better reflector continuity. The concave structure is accurately imaged, confirming the superiority of the inverted model and the effectiveness of the multi-scale FWI.

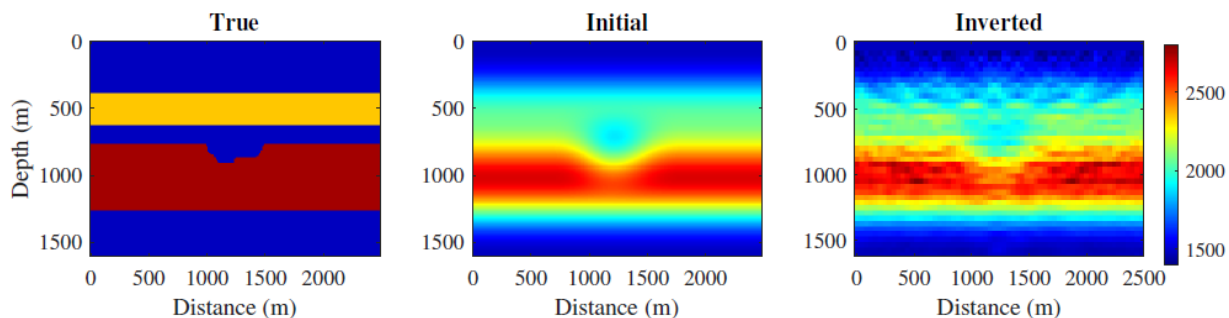


Figure 4. Single-scale FWI performed over 5 iterations in the frequency range of 1-25 Hz.

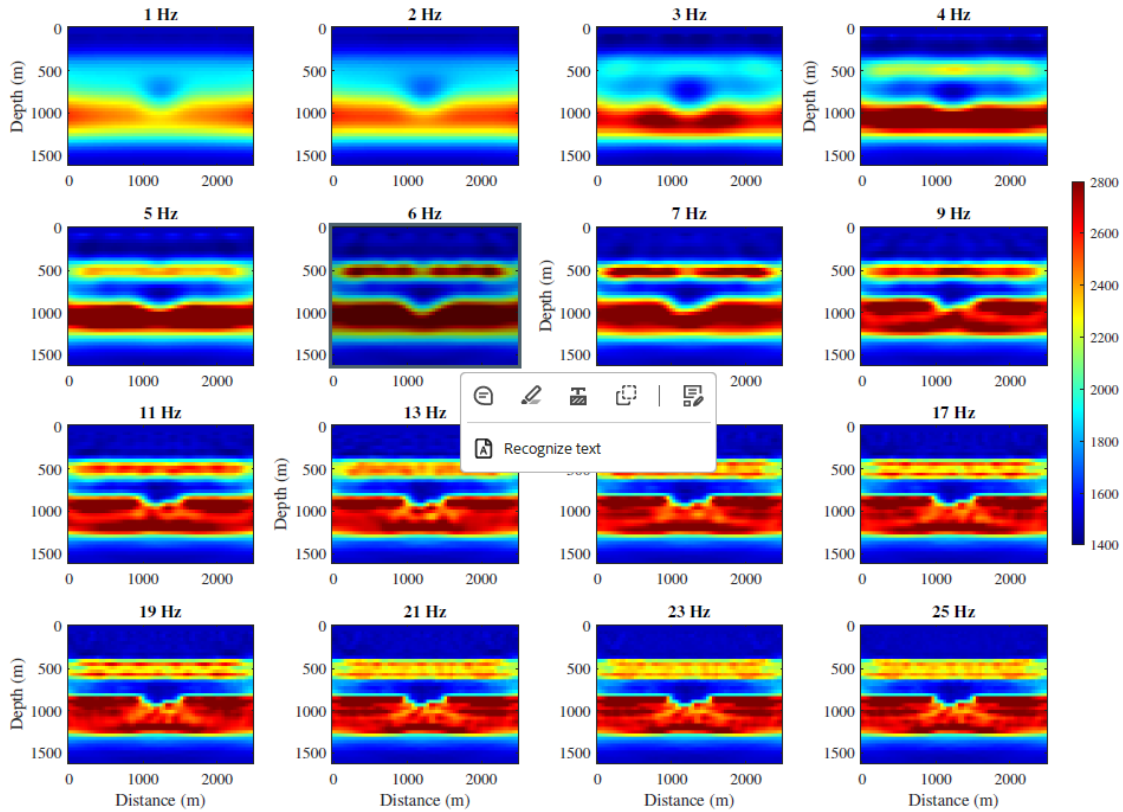


Figure 5. Multiscale FWI ranging from 1 Hz to 25 Hz, conducted over 5 iterations.

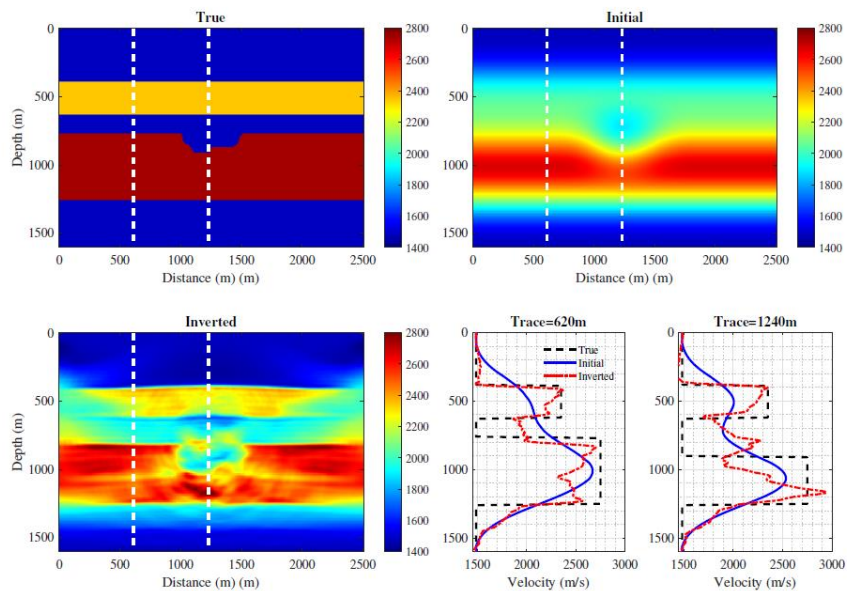


Figure 6. Multiscale FWI results conducted over 16 iterations. The true, initial, and inverted velocity models are shown, along with velocity profiles at trace locations $x = 620\text{m}$ and $x = 1240\text{m}$, highlighting the improvements in resolution and accuracy achieved by the inversion.

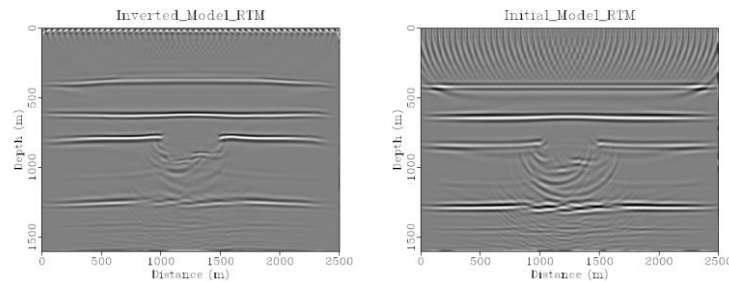


Figure 7. RTM based on the initial model (see in Figure 4) and inverted velocity model (see in Figure 6).

CONCLUSIONS

This study systematically evaluated the performance of FWI on synthetic data generated from a physical modeling facility channel model. The multiscale frequency domain approach demonstrating that: Low-frequency data are essential for resolving large-scale channel structures and stabilizing the inversion process; A progressive incorporation of frequency bands improves the recovery of fine-scale details and structural boundaries resulting in a high resolution velocity model: The results demonstrate the development of an integrated, user-friendly, and efficient FWI code that is adaptable to various types of models. Additionally, the findings highlight the robustness of multiscale FWI in addressing both large-scale and detailed subsurface imaging challenges. Future work will focus on applying these workflows to actual physical modeling data to further validate the methodologies and explore their broader applicability.

Acknowledgements

The sponsors of CREWES are gratefully thanked for continued support. This work was funded by CREWES industrial sponsors, and NSERC (Natural Science and Engineering Research Council of Canada) through the grant CRDPJ 543578-19. Further support of this work was provided by Emissions Reduction Alberta through the ACT4-SPARSE project.

References

- Huang, R., Zhang, Z., Wu, Z., Wei, Z., Mei, J., and Wang, P., 2021, Full-waveform inversion for full-wavefield imaging: Decades in the making: *The Leading Edge*, 40, No. 5, 324-334.
- Lailly, P., and Bednar, J., 1983, The seismic inverse problem as a sequence of before stack migrations, in *Conference on inverse scattering: theory and application*, vol. 1983, Philadelphia, Pa, 206-220.
- Pan, W., Innanen, K. A., and Wang, Y., 2020, Parameterization analysis and field validation of VTI-elastic full-waveform inversion in a walk-away vertical seismic profile configuration: *Geophysics*, 85, No. 3, B87-B107.
- Pratt, R. G., 1990, Frequency-domain elastic wave modeling by finite differences: A tool for cross-hole seismic imaging: *Geophysics*, 55, No. 5, 626-632.
- Tarantola, A., 1984, Inversion of seismic reflection data in the acoustic approximation: *Geophysics*, 49, No. 8, 1259-1266.
- Vigh, D., Cheng, X., Xu, J., and Jiao, K., 2023, Forge ahead in acquisition and model building via full-waveform inversion: Gulf of Mexico case study: *Geophysics*, 88, No. 5, B285-B295.
- Virieux, J., and Operto, S., 2009, An overview of full-waveform inversion in exploration geophysics: *Geophysics*, 74, No. 6, WCC1-WCC26.
- Yang, P., Gao, J., and Wang, B., 2015, A graphics processing unit implementation of time-domain full-waveform inversion: *Geophysics*, 80, No. 3, F31-F39.